Core-Size-Dependent Catalytic Properties of Bimetallic Au/Ag Core–Shell Nanoparticles
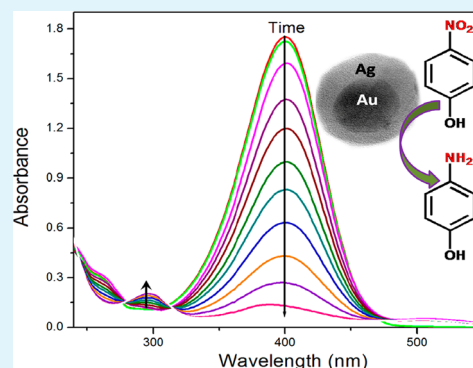
Krishna Kanta Haldar, Simanta Kundu, and Amitava Patra*

Department of Materials Science, Indian Association for the Cultivation of Science, Jadavpur, Kolkata 700032, India

S *Supporting Information*

ABSTRACT: Bimetallic core–shell nanoparticles have recently emerged as a new class of functional materials because of their potential applications in catalysis, surface enhanced Raman scattering (SERS) substrate and photonics etc. Here, we have synthesized Au/Ag bimetallic core–shell nanoparticles with varying the core diameter. The red-shifting of the both plasmonic peaks of Ag and Au confirms the core–shell structure of the nanoparticles. Transmission electron microscopy (TEM) analysis, line scan EDS measurement and UV–vis study confirm the formation of core–shell nanoparticles. We have examined the catalytic activity of these core–shell nanostructures in the reaction between 4-nitrophenol (4-NP) and $NaBH_4$ to form 4-aminophenol (4-AP) and the efficiency of the catalytic reaction is found to be increased with increasing the core size of Au/Ag core–shell nanocrystals. The catalytic efficiency varies from 41.8 to 96.5% with varying core size from 10 to 100 nm of Au/Ag core–shell nanoparticles, and the Au_{100}/Ag bimetallic core–shell nanoparticle is found to be 12-fold more active than that of the pure Au nanoparticles with 100 nm diameter. Thus, the catalytic properties of the metal nanoparticles are significantly enhanced because of the Au/Ag core–shell structure, and the rate is dependent on the size of the core of the nanoparticles.

KEYWORDS: *nanoparticle, core–shell, Au/Ag, catalytic properties*

INTRODUCTION

Bimetallic nanoparticles have aroused intensive interest because of their fascinating optical, electronic, sensing and catalytic properties.[1−4] Some unique physiochemical and surface characteristics are evolved in bimetallic nanoparticles due to combinational interactions between two metallic electronic states which are different from individual metals. Properties of monometallic nanoparticles have been extensively studied with various morphologies, sizes and shapes.[5−7] The bimetallic nanostructures can have various architectures including alloy, nanowires, dendrite, and core–shell etc.[8−12] Among these nanostructures, bimetallic core–shell nanostructure of gold and silver have attracted a lot of interest for their plasmonic, catalytic and sensor based applications.[13−17] Yang et al.[18] have demonstrated Au–Ag and Ag–Au bimetallic core–shell nanoparticles for SERS application. Physiochemical properties of this bimetallic core–shell nanoparticles solely depends on the dimension of core and shell and on the composition.[19] There are several reports on the modification of physiochemical properties by shell thickness variation of Au/Ag core–shell nanoparticles. Pande et al.[20] have been demonstrated the influence of shell thickness of Au–Ag core–shell nanoparticles on SERS. Samal et al.[15] have reported the synthesis and modulation of SERS properties of Au–Ag core–shell nanoparticles by tuning the shell thickness and the size of the Au core. Thus, the SERS activity of the Au–Ag core–shell nanoparticles can be tuned by the modification of core and shell dimension.

In spite of SERS application of the bimetallic nanoparticles, catalytic application is found to be interesting. The catalytic properties can be tuned by tuning the size and shape of the nanoparticles.[21] Recently, Xia et al.[22] have reported the comparative catalytic activity of the Au nanoparticles, nanoboxes, and nanocages by reduction of nitrophenols. Again, the catalytic property can be tuned with changing the nanoparticle composition from single component to bimetallic. Meng et al.[1] have demonstrated the Au/Ag bimetallic dendrite nanostructurs for efficient catalytic applications. Lei et al.[23] have reported the enhanced catalytic activity of Au–Ag nanoplates for the reduction of nitrophenols. Among the different morphologies, the core–shell type nanoparticles are most interesting as the core diameter and the shell thickness might play important role on the catalytic activity. Recently, Tsao et al.[21] have demonstrated the shape dependent catalytic activity of the Au–Ag core–shell nanocrystals. Thus, the catalytic and other physiochemical activities of the core–shell materials can be tuned by changing the size of the core in core–shell structures. To the best of our knowledge, little attention has

Table 1. Detail Conditions for the Synthesis of Different Sized Au/Ag Bimetallic Core−Shell Nanoparticles

		volume (mL)					
size of Au seeds (nm)	concentration of Au NP (NPs/mL)	AgNO$_3$ (0.1 mM)	β-CD (0.05 mM)	PVP (0.1%)	cysteine (0.05 mM)	pH	T (°C)
~10	1.2×10^{12}	3	1.5	0.65	1.5	~10	85−90
~20	5.5×10^{11}	3	1.5	0.65	1.5	~10	85−90
~40	1.8×10^{11}	3	1.5	0.65	1.5	~10	85−90
~60	9.6×10^{10}	3	1.5	0.65	1.5	~10	85−90
~80	5.7×10^{10}	3	1.5	0.65	1.5	~10	85−90
~100	4.3×10^{10}	3	1.5	0.65	1.5	~10	85−90

been paid on the influence of core size on the catalytic activity of the core−shell bimetallic nanoparticles.

In the present study, we have prepared Au/Ag core−shell nanomaterials by a simple method. We have tuned the diameter of the core material with a fixed shell thickness. Finally, we have evaluated the catalytic properties of Au/Ag based nanostructures (including bimetallic and monometallic nanoparticles) using a model reaction based on the reduction of 4-nitrophenol to aminophenol by NaBH$_4$.

EXPERIMENTAL PROCEDURE

Materials. Chloroauric acid (HAuCl$_4$.3H$_2$O, 99.9%), silver nitrate (99.99%), β-cyclodextrin (β-CD; Fluka), cysteine (Lobachemie), polyvinylpyrrolidone (PVP), trisodium citrate, 4-nitrophenol, and sodium borohydride (NaBH$_4$) were purchased from Merck India Ltd. All of the reagents were used without further purification. Deionized (DI) water (18 MΩ) was used in all the experiments.

Synthesis of Different-Sized Au Nanoparticles. Gold nanoparticles of 10, 20, 40, 60, 80, and 100 nm diameter were synthesized by a reported method with some modifications.[24] Typically, a solution of 1.25 mL of 10 mM chloroauric acid (HAuCl$_4$, 3H$_2$O) in Milli-Q water (46.25 mL) was heated with a heating mantle in a (100 mL) two-necked round-bottomed flask for 30 min under vigorous stirring. A condenser was utilized to prevent the evaporation of the solvent. After that, a solution of 2.5 mL of trisodium citrate (1%) was injected. The color of the solution has changed from yellow to bluish gray and then to soft pink in 10 min. For this particular procedure, the Au nanoparticles were about 10−12 nm in diameter. For sake of simplicity, the gold concentration was expressed with reference to its chloroauric acid precursor, which was assumed to be converted completely into Au nanoparticles during the NP synthesis. The resulting particles (~10 nm, ~1.2×10^{12} NPs/mL) are coated with negatively charged citrate ions and hence are well suspended in H$_2$O. This gold seeds were used for the preparation of larger size 20, 40, 60, 80, and 100 nm Au nanoparticles by seeded growth method, respectively. These nanoparticle solutions were centrifuged and washed several times and then redispersed in required volume of deionized water. These stock solutions were further used for the Au/Ag core−shell nanoparticle preparation.

Synthesis of Au/Ag Bimetallic Core−Shell Nanoparticles. Au/Ag bimetallic core−shell nanoparticles were synthesized using PVP, cystein and cyclodextrin. Several experiments and control synthesis were preliminary performed to optimize the conditions for the synthesis of Au/Ag bimetallic core−shell nanocrystal. Details of these experiments are given in the Supporting Information. Water-soluble and stable Au/Ag core−shell nanostructures were fabricated by a simple colloidal approach. In brief, 0.65 mL of 0.1% polyvinylpyrrolidone (PVP) was mixed with 7 mL of the prepared Au NP stock solutions with vigorous stirring for 20 min to modify the gold nanoparticle surfaces and stabilization of the nanoparticles. Now, an appropriate amount of β-cyclodextrin (1.5 mL, 0.05 mM) and cysteine (1.5 mL, 0.05 mM) were mixed to above solution and the solution was stirred for few minutes to mix completely. The pH of the solution was adjusted to ~10 by adding NaOH solution and the solution was allowed to incubate for 15 min.

After that the mixture was kept on a water bath at 85 °C. Then, AgNO$_3$ solution (3 mL, 0.1 mM) was added dropwise to this mixture with constant stirring. With each addition, the pink color of gold NPs changes and finally leads to a bright yellow color of silver NPs after 30 min, indicating the formation of Ag shell on the Au particles. Similarly, we have synthesized bimetallic core−shell nanoparticles with 20 nm, 40 nm, 60 nm, and 80 and 100 nm Au nanoparticles. We have maintained the same shell thickness (~10 nm) for all the core−shell nanoparticles. There are two ways to fix the shell thickness of a core/ shell with different core sizes, either by increasing the concentration of shell materials keeping particle concentration same, or by decreasing the particle concentration of bigger size core materials. In our case, we have decreased the seed particle concentration for the larger seed sizes maintaining the equal volume of silver nitrate solution, to maintain the ~10 nm shell thickness of Ag in the Au/Ag core−shell nanoparticles. The details condition used in the synthesis are summarized in Table 1 and also a flowchart for the synthesis of core−shell is given in the Supporting Information.

Characterization. Absorption spectra of the as synthesized metallic nanoparticles and bimetallic core−shell nanocrystals, were taken at room temperature with a Shimadzu UV-2450 UV−vis spectrometer. High-resolution transmission electron microscope (HR-TEM) images were taken using JEOL, JEM-2100F at an operating voltage of 200 kV. STEM-Dark Field images were taken by JEOL, JEM-2100F. EDS spectrum and High Resolution Real-time Line Scan data were collected with the help of Oxford INCA x-sight X-ray analyzer attached to UHR FEG-TEM (JEOL, JEM-2100F).

Catalytic Measurements. Two hundred microliters of 0.015 M 4-nitrophenol solution was added to 30 mL of DI H$_2$O (18MΩ). Then, 1 mL of 0.01 M NaBH$_4$ solution was added, resulting in the change of the solution's color from color-less to bright yellow. Finally, ~1.5 mL containing 6.3×10^8 Au nanoparticles or Au/Ag nanostructures was added from stock solutions and the mixture was stirred for a few seconds (we have maintained the same particle concentration of the catalyst core−shell NPs during the catalytic reaction to compare all the catalytic experiments using different core−shell NPs). Absorption measurements were conducted by taking 1 mL aliquots from the solution and recording their absorption spectrum between 200 and 600 nm. Time difference between the absorption measurements were 1 min.

RESULTS AND DISCUSSION

The shell thickness of the bimetallic core−shell nanoparticles can be controlled by simply adjusting a few synthesis parameters. Our synthetic strategy relies on combining two key concepts, first, the use of Au nanoparticles as the core seeds for Ag coating; second, a suitable temporal variation of the surfactant composition in the reaction mixture during the synthesis. Citrate capped Au nanoparticles with spherical shape were first prepared by using modified literature protocols.[24] The formation of heterostructures is achieved by keeping the PVP: cysteine: Au molar ratio from 1:1:5 to 1:1:14 (while the Ag concentration was fixed). The alkalinity of the gold colloidal solution helps to induce the slow chemical reduction of Ag (I) ions and their deposition on the gold particles. Slower rate of reduction by β-cyclodextrin is preferred because it prevents the

21947

dx.doi.org/10.1021/am507391d | ACS Appl. Mater. Interfaces 2014, 6, 21946−21953

formation of pure Ag aggregates and produces a uniform silver shell over Au seeds.[25] The pink color of gold NPs changes gradually with the addition of $AgNO_3$ solution and finally produces bright yellow color of silver NPs. Several controlled experiment were performed for the standardization of the synthesis which are discussed in the Supporting Information in detail (Figures S1 and S2). The growth of silver shell was monitored recording UV−vis spectrum. Figure 1 shows the
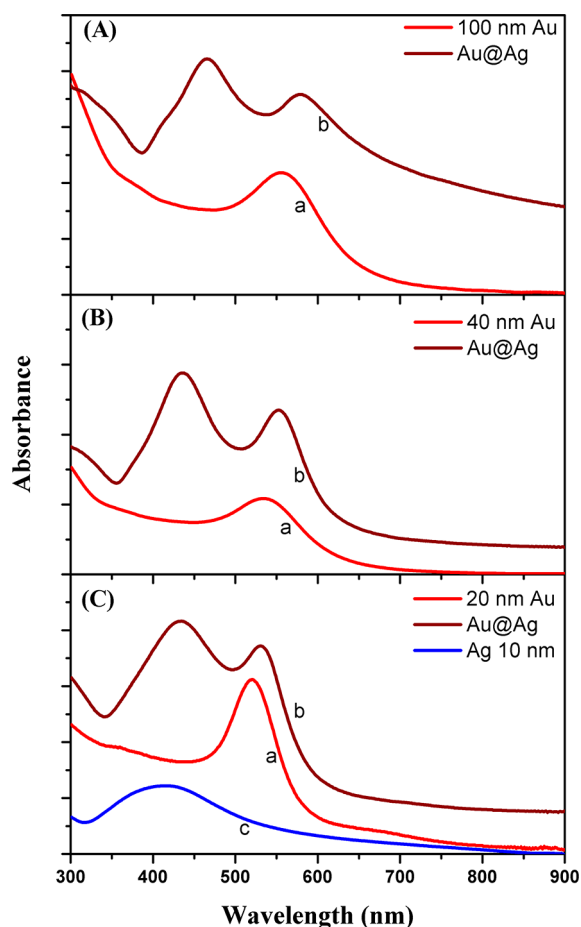

Figure 1. UV spectra of (A) 20, (B) 40, and (C) 100 nm Au nanoparticles (a plots) and corresponding Au/Ag bimetallic core−shell nanoparticles with 10 nm shell thickness (b plots) and Ag nanoparticle of 10 nm diameter (c plot in panel C).

UV−vis spectra of the Au nanoparticles with diameter of 20, 40, and 100 nm and the corresponding core−shell nanoparticles

with a fixed shell thickness of ∼10 nm. The red shifting of the absorption band from 520 to 561 nm of Au is observed with changing the Au particle size from 10 to 100 nm which is in consistent with previous result.[26] The absorption band at 520 nm corresponds to the surface plasmon resonance of Au nanoparticles. The main dipolar resonance band is red-shifted and broaden when the diameter of Au NP further increases. It can be seen from the UV−vis spectra that core−shell nanoparticles show a double peak spectral line pattern, which is the characteristic plasmonic feature of Au/Ag core−shell nanoparticles.[27,28]

As the size of the Au core increases with a fixed 10 nm Ag shell, the absorption peak corresponding to the Au plasmon is gradually red-shifted from the pure Au peaks. This red shifting of the Au plasmon because of core−shell formation is in consistent with the previous reports.[27] The plasmon peak corresponding to Ag is also red-shifted with the increase of core diameter though the thickness of the Ag shell is same for all the samples. This red shifting may be attributed to the increase of number of Ag atoms in each core−shell to maintain the fixed shell thickness with increasing core diameter. Thus, the double peak spectral line pattern in the UV−vis spectra and the red shifting of both the Au and Ag band in the Au/Ag heterostructure indicate that these heterostructures are not a simple physical mixture of two different kinds of metal particles, rather they depict a synergistic optical features of bimetallic core−shell nanoparticles, which is in consistent with previous results.[25]

Structural Analysis of Au/Ag Bimetallic Core−Shell Nanoparticles. Structural analysis of the synthesized nanoparticles has been characterized by TEM measurement. The Au nanoparticles are synthesized by seed mediated growth method. The TEM images of the core Au nanoparticles with diameter of 20 (± 4) nm, 40 (± 5) nm and 100 (± 10) nm are shown in the Supporting Information Figure S3. We have synthesized Au/Ag core−shell bimetallic nanoparticles with the core diameter varying from 10 to 100 nm and the shell thickness is fixed at ∼10 nm. Figure 2 shows the TEM images of the bimetallic core−shell nanoparticles of Au_{20}/Ag, Au_{40}/Ag, and Au_{100}/Ag. The core−shell nature of the nanoparticles can be seen from the TEM images.

To get structural details of the heterostructure nanoparticles and to confirm the core−shell type structure formation, we performed HRTEM, EDS analysis, and elemental mapping. Figure 3 represents the TEM, HAADF-STEM, and elemental mapping images of the bimetallic core−shell nanoparticles of Au_{100}/Ag. It is seen from the TEM image (Figure 3A), that the
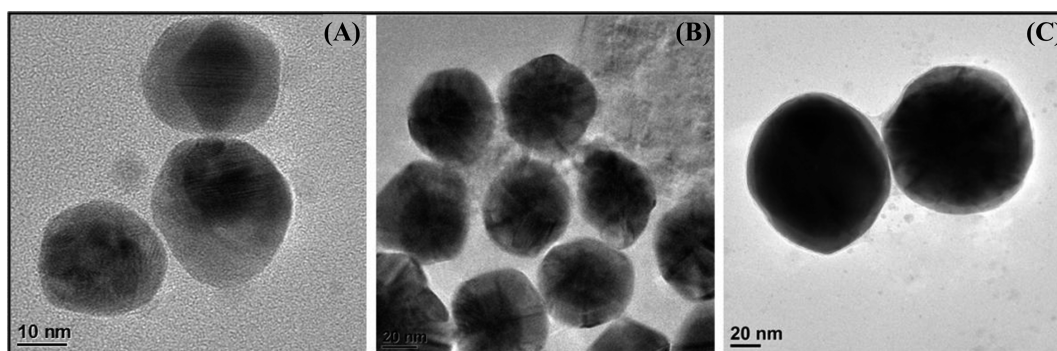

Figure 2. TEM images of (A) Au_{20}/Ag, (B) Au_{40}/Ag, and (C) Au_{100}/Ag bimetallic core−shell nanoparticles.
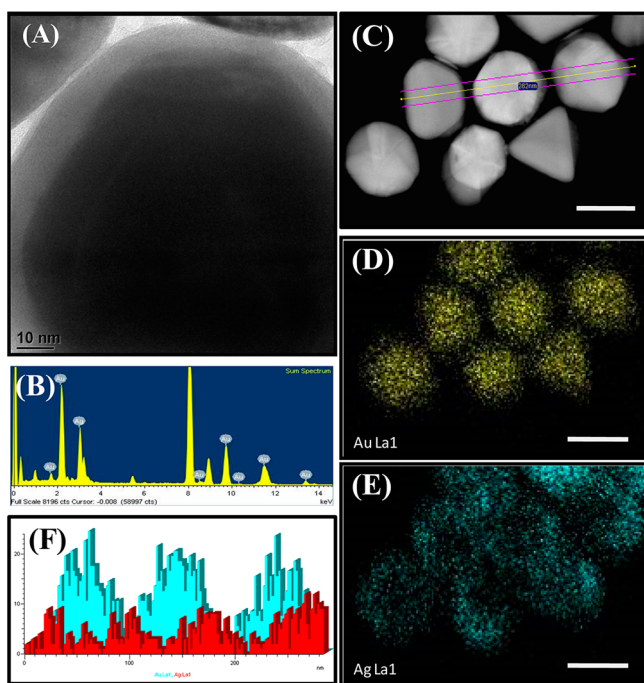
Figure 3. (A) TEM image, (B) EDAX spectra, (C) STEM−dark field image, (D, E) corresponding element mapping images of Au_{100}/Ag bimetallic core−shell NP (scale bar in C−E is 100 nm), and (F) EDAX line scan representing Au (cyan) and Ag (red) shown in panel C.

core−shell nanoparticle is in uniform orientation, indicating the single crystalline structure of the core−shell bimetallic nanoparticles. Similar observations have been made in case of Pt-group metal core−shell nanoparticle derived from the reduction of using different reducing agents,[29,30] indicating the formation of core−shell nanoparticle phase. To further confirm the core−shell structure of Au/Ag bimetallic nanoparticles, HAADF-STEM-EDS analysis is performed (Figure 3B), which confirms the presence of both Au and Ag metals within the nanoparticles.

To investigate the distribution of the Au and Ag metals in the core−shell structure, we have carried out elemental mapping. Figure 3C shows the STEM−dark-field image of the Au100/Ag core−shell nanoparticles. Images D and E in Figure 3 show the distribution of Au and Ag atoms for the Au_{100}/Ag core−shell nanoparticles of Figure 3C. From the distribution of Au and Ag in the nanoparticles it can be clearly seen that the Au atoms are mostly concentrated in the center of the nanoparticles, whereas the Ag atoms are situated on the circumference of the nanoparticles. This clearly indicates the formation of almost homogeneous core−shell structure of the synthesized Au/Ag heterostructures. To confirm the core−shell type of structure of the nanoparticles, we have taken high-resolution real-time line scan data (Figure 3F) across the nanoparticles as shown by the yellow highlighted line in the STEM- Dark Field image of Figure 3C. It is seen from line scan data that the X-ray intensity of the Au is maximum and Ag is minimum in the core region. At the edge of the particles, the X-ray intensity of Ag is maximum and no X-ray intensity of the Au. Thus, the line scan profile of the nanoparticle is in agreement with the core−shell structures of the nanoparticles.

It is proposed that the formation of bimetallic core/shell nanoparticle involves a slow nucleation and fast autocatalytic

reduction process.[31−36] Moreover, in the presence of seed, the formation of bimetallic core/shell nanoparticle followed a seed-assisted growth mechanism, which follows both homogeneous and heterogeneous nucleation of metal atoms and Ostwald ripening growth.[37] In the present work, similar type of evolution of Au/Ag NCs was observed, which was investigated by taking aliquots out of the reaction system at various stages to understand the formation mechanism of Au/Ag bimetallic core/shell nanoparticle. These are discussed in detail in the Supporting Information (Figure S4).

Catalytic Property of Au/Ag Bimetallic Core−Shell Nanoparticles. To monitor the effect of core size on the physical properties, we have examined the catalytic activities of Au/Ag core−shell nanoparticles in the reaction of 4-nitrophenol (4-NP) with $NaBH_4$ to form 4-aminophenol (4-AP). The conversion from 4-NP to 4-AP occurs via an intermediate 4-nitrophenolate ion formation.[38] It is known that this reaction does not occur in the absence of catalysts. The reduction of 4-NP to 4-AP in aqueous $NaBH_4$ is thermodynamically favorable (E_0 for 4-NP/4-AP = −0.76 V and $H_3BO_3/BH_4^- = -1.33$ V versus NHE).[39] The large potential difference between the donor and the acceptor molecule exhibits kinetic barrier. Metal nanoparticles are known[40] to catalyze this reaction by facilitating electron transfer from the donor BH_4^- to acceptor 4-NP. We have monitored the progress of the reaction by measuring the absorption spectrum of 4-nitrophenol and 4-aminophenol as a function of time. With the addition of the catalyst bimetallic Au/Ag hybrid core−shell nanoparticles to the reaction mixture containing 4-NP and $NaBH_4$, a gradual decrease in the characteristic absorption peak of 4-nitrophenol at 400 nm and an evolution of a new peak for 4-aminophenol at 298 nm is observed. Figure 4a shows the absorption spectra of the reaction mixture at different time intervals of the reaction. It is seen from the spectrum that the intensity of the absorption peak of 4-NP decreases to almost zero within 11 min. In a control experiment, where 4-nitrophenol and $NaBH_4$ are used without using any catalyst, the intensity of the typical absorption peak of 4-nitrophenol at 400 nm changes very little (see Figure S5A in the Supporting Information), indicating that 4-nitrophenol is not reduced by only $NaBH_4$. Also, there is no significant change in absorption band of 4-NP in the presence of pure 10 nm Ag nanoparticle (shown in Figure S5B in the Supporting Information) and pure Au nanoparticles (see Figure S5C in the Supporting Information), indicating no reduction of 4-NP. Thus, pure Au or Ag nanoparticles are unable to catalyze the reaction. Au/Ag core−shell nanoparticles are played a significant role in the catalysis of 4-NP to 4-AP. It is to be noted that the efficiency of the catalytic reaction increases with increasing the core size of Au in Au/Ag core−shell nanocrystals. The efficiency of the catalytic reaction are 41.8, 49.5, 61.4, 73.2, 81.7, and 96.5% for Au_{10}/Ag, Au_{20}/Ag, Au_{40}/Ag, Au_{60}/Ag, Au_{80}/Ag, and Au_{100}/Ag core−shell nanoparticles, respectively. It takes ~11 min time to complete reduction of the 4-nitrophenol to 4-aminophenol for Au_{100}/Ag core−shell nanoparticles. The reduction kinetics of the experiments without any catalyst, with 100 nm Au NP, 10 nm Ag NP and Au_{100}/Ag core−shell NP as catalyst are shown in Figure S6 in the Supporting Information, which describe the ratio of the absorption peak intensity of 4-nitrophenol at a given time to the absorption intensity at initial stage. A sharp decrease in the 4-nitrophenol concentration can be seen when Au_{100}/Ag bimetallic core−shell is used as the catalyst.
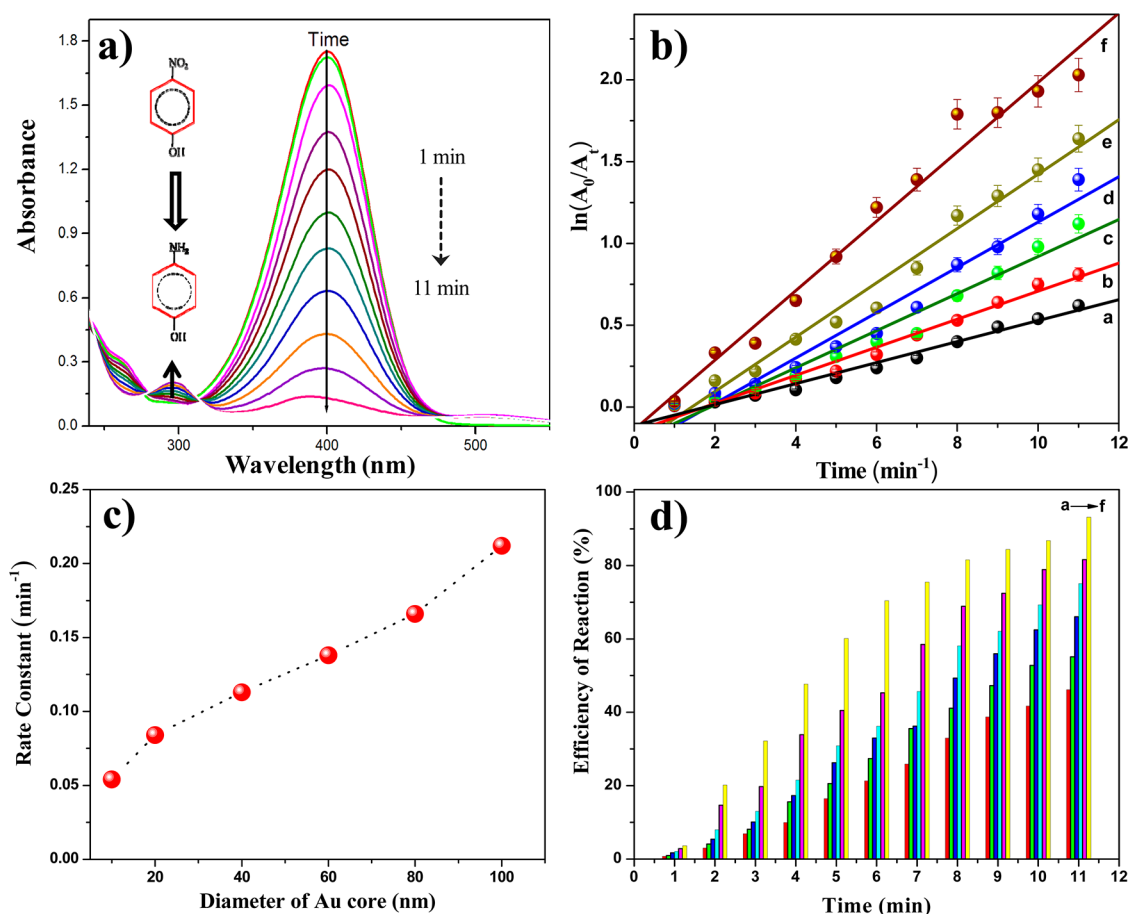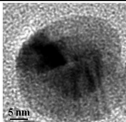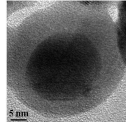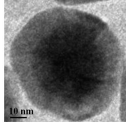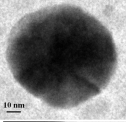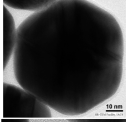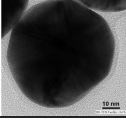
Figure 4. (a) Absorption spectra of 4-nitrophenol reduced by NaBH₄ in the presence of Au$_{100}$/Ag core−shell nanoparticles with 1 min time interval; (b) ln(A_o/A_t) vs time plot for determination of rate constants of core−shell nanoparticles with core diameter (a) 10, (b) 20, (c) 40, (d) 60, (e) 80, and (f) 100 nm; (c) plot of catalytic reaction rate constant vs core diameter; and (d) catalytic reaction efficiency of bimetallic core−shell NP with increasing core diameter (a) 10, (b) 20, (c) 40, (d) 60, (e) 80, and (f) 100 nm.

The rate of catalysis of 4-NP reduction increases gradually with the increase of size of the pure Au nanoparticle size (see the Supporting Information Table S1). However, the catalytic activity of pure Au is very low compared to their corresponding Au/Ag core−shell bimetallic nanoparticles (Table 2). Qiang Xu et al.[41] have reported that the catalytic activity of Au@Co bimetallic core/shell is much higher than pure Au, pure Co and AuCo alloy. In the present study, the PVP molecule is being used for the stabilization of Au nanoparticles and Au has strong affinity to PVP molecules.[42] The significant decrease of the catalytic efficiency of PVP-stabilized Au or Ag nanoparticles is due to surface coverage by PVP, bulky polymer which hinders the diffusion of reactants molecules toward the Au or Ag nanoparticles which is consistent with previous results.[43] During core−shell formation, it is believed that PVP molecules are replaced by a complex exchange mechanism. The improved catalytic activity of Au/Ag bimetallic core−shell can be attributed to the electronic effect and their unique structure. The electronic effect, also termed as "ligand effect", can originate from the heterometallic bonding on or near the surface, which has been widely reported in a number of catalytic reactions based on the bimetallic nanoparticles.[44−49] To compare the catalytic activities of Au/Ag bimetallic core−shell nanoparticles with different sizes of Au core, we have calculated the reaction rate constants by measuring the absorbance (A) of absorption peak of 4-NP at 400 nm with

reaction time and plotting ln(A_o/A_t) versus reaction time (t). As shown in Figure 4b, a linear relationship between ln(A_o/A_t) and reaction time (t) is obtained for all the catalysts, indicating the reaction is first-order with respect to 4-nitrophenol. The rate constants (k) are measured from the slope of the lines and the values are 0.054, 0.084, 0.113, 0.138, 0.166, and 0.212 min^{-1} for Au$_{10}$/Ag, Au$_{20}$/Ag, and Au$_{40}$/Ag, Au$_{60}$/Ag, Au$_{80}$/Ag, and Au$_{100}$/Ag core−shell nanoparticles, respectively. The activity of Au$_{100}$/Ag core−shell nanoparticles is 2.5 times higher than Au$_{10}$/Ag core−shell nanoparticles. This result demonstrates a clear dependence of activity on the core size of the bimetallic core−shell nanoparticles (Figure 4c, d). Also the Au/Ag core−shell nanoparticles manifest a much higher activity than monometallic Au or Ag counterpart. It is important to note that Au$_{100}$/Ag bimetallic core−shell nanoparticles are 12-fold more active than that of the corresponding 100 nm size of Au nanoparticles in terms of activity per mass of catalyst (Table 2 and Table S1 in the Supporting Information). Thus, Au$_{100}$/Ag bimetallic core−shell nanoparticle exhibits a great potential in catalytic applications. The significant enhancement in the catalytic activity of the Au/Ag bimetallic core−shell nanoparticles can be attributed to the following reasons. First, composition and size of bimetallic core−shell nanoparticles may enhance the catalytic effect.[50] It is known that surface area plays an important role on catalytic property. Here, the calculated surface area of 100 nm Au NP is 23.8 times higher

Table 2. Catalytic Reaction Efficiency and the Rate Constant of the 4-Nitrophenol Reduction by Au/Ag Bimetallic Core−Shell Nanoparticles

System		Reaction efficiency (%)	Rate constant (min⁻¹)
10 nm core Au@Ag		41.8	0.054
20 nm core Au@Ag		49.5	0.084
40 nm core Au@Ag		61.4	0.113
60 nm core Au@Ag		73.2	0.138
80 nm core Au@Ag		81.7	0.166
100 nm core Au@Ag		96.5	0.212

than 10 nm Au NP and the surface area of Au_{100}/Ag bimetallic core/shell NPs is 1.44 times higher than monometallic 100 nm Au NPs. Thus, if surface area is only factor then the catalytic activity of Au_{100}/Ag bimetallic core/shell NPs must be comparable with 100 nm sizes Au NP. An exact mechanism for this interesting catalytic behavior of such bimetallic nanoparticle is still in debate.

Another probable reason for enhancement of the catalytic activity may be due to the increase in capacitance in the core−shell nanoparticles. As the Fermi level for gold (−5.0 eV) is situated at lower energy than that for silver (−4.6 eV), thus the gold atoms in the core can have a strong electronic effect on the surface silver atoms by electron transfer.[18] Thus, an increase in the electron density on the surface of the bimetallic Au/Ag core−shell nanoparticles can improve the catalytic activity.[49,51] This increase of electron density can be correlated with the enhancement of charge capacitance due to core−shell structure, because capacitance value within the heterostructure increases with increasing the size of the core. To estimate the capacitance (C) of the core−shell particles, we used the following equation

$$C = 4\pi\varepsilon_0\varepsilon(r/d)(r + d) \qquad (1)$$

where r is the radius of the Au core, d is the fixed shell thickness of 10 nm, ε_0 is the dielectric constant at vacuum, ε is the static dielectric constant of the shell which we take 2.25,[52] and the capacitance values are 212, 565, 1696, 3391, 5652, and 8478 aF (atto Farad) for Au_{10}/Ag, Au_{20}/Ag, Au_{40}/Ag, Au_{60}/Ag, Au_{80}/Ag, and Au_{100}/Ag core−shell nanoparticles, respectively. It indicates that more electrons are needed to raise Fermi level for higher capacitance value. It reveals that the diameter of core of bimetallic core−shell nanoparticles controls the charge capacitance value. These results indicate that the catalytic

performance of Au/Ag nanoparticle could be greatly enhanced by controlling both the core and shell structures.

CONCLUSION

Here, we have synthesized Au/Ag core−shell bimetallic nanoparticles with varying core size of these nanoparticles. Detailed TEM analysis and UV−vis study confirm the formation of core−shell nanoparticles. In the present study, we demonstrate the core size dependent catalytic properties of Au/Ag core−shell nanoparticles and surface enhanced Raman properties of Au/Ag core−shell nanoparticles. The efficiency of the catalytic reaction varies from 41.8 to 96.5% with varying core size from 10 to 100 nm. It reveals that the catalytic performance is significantly enhanced by controlling core size. Thus, Au/Ag bimetallic core−shell nanoparticles are found to be suitable for efficient catalytic applications.

ASSOCIATED CONTENT

ⓈSupporting Information

Flowchart for the synthesis of core−shell nanoparticles and detailed controlled experiments, TEM images of pure Au nanoparticles, TEM images sampled at different conditions during the core/shell formation, absorption spectra of different controlled catalytic reactions, catalytic activities of different catalytic reactions, and catalytic reaction efficiency values for different sized Au NPs. This material is available free of charge via the Internet at http://pubs.acs.org.

AUTHOR INFORMATION

Corresponding Author
*E-mail: msap@iacs.res.in. Phone: (91)-33-2473-4971. Fax: (91)-33-2473-2805.

■ REFERENCES

(1) Huang, J.; Vongehr, S.; Tang, S.; Lu, H.; Shen, J.; Meng, X. Ag Dendrite-Based Au/Ag Bimetallic Nanostructures with Strongly Enhanced Catalytic Activity. *Langmuir* **2009**, *25*, 11890−11896.

(2) Mizukoshi, Y.; Fujimoto, T.; Nagata, Y.; Oshima, R.; Maeda, Y. Characterization and Catalytic Activity of Core−Shell Structured Gold/Palladium Bimetallic Nanoparticles Synthesized by the Sono-chemical Method. *J. Phys. Chem. B* **2000**, *104*, 6028−6032.

(3) Nishida, N.; Shiraishi, Y.; Kobayashi, S.; Toshima, N. Fabrication of Liquid Crystal Sol Containing Capped Ag−Pd Bimetallic Nanoparticles and Their Electro-Optic Properties. *J. Phys. Chem. C* **2008**, *112*, 20284−20290.

(4) Shon, Y.-S.; Dawson, G. B.; Porter, M.; Murray, R. W. Monolayer-Protected Bimetal Cluster Synthesis by Core Metal Galvanic Exchange Reaction. *Langmuir* **2002**, *18*, 3880−3885.

(5) Jin, R.; Charles Cao, Y.; Hao, E.; Metraux, G. S.; Schatz, G. C.; Mirkin, C. A. Controlling Anisotropic Nanoparticle Growth through Plasmon Excitation. *Nature* **2003**, *425*, 487−490.

(6) Sun, Y.; Xia, Y. Shape-Controlled Synthesis of Gold and Silver Nanoparticles. *Science* **2002**, *298*, 2176−2179.

(7) Jena, B. K.; Raj, C. R. Synthesis of Flower-like Gold Nanoparticles and Their Electrocatalytic Activity Towards the Oxidation of Methanol and the Reduction of Oxygen. *Langmuir* **2007**, *23*, 4064−4070.

(8) Zhang, Q.; Xie, J.; Lee, J. Y.; Zhang, J.; Boothroyd, C. Synthesis of Ag@AgAu Metal Core/Alloy Shell Bimetallic Nanoparticles with Tunable Shell Compositions by a Galvanic Replacement Reaction. *Small* **2008**, *4*, 1067−1071.

(9) Selvakannan, P. R.; Sastry, M. Hollow Gold and Platinum Nanoparticles by a Transmetallation Reaction in an Organic Solution. *Chem. Commun.* **2005**, 1684−1686.

(10) Yang, J.; Lee, J. Y.; Too, H.-P.; Valiyaveettil, S. A Bis(p-sulfonatophenyl)phenylphosphine-Based Synthesis of Hollow Pt Nanospheres. *J. Phys. Chem. B* **2005**, *110*, 125−129.

(11) Teng, X.; Wang, Q.; Liu, P.; Han, W.; Frenkel, A. I.; Wen; Marinkovic, N.; Hanson, J. C.; Rodriguez, J. A. Formation of Pd/Au Nanostructures from Pd Nanowires via Galvanic Replacement Reaction. *J. Am. Chem. Soc.* **2007**, *130*, 1093−1101.

(12) Shore, M. S.; Wang, J.; Johnston-Peck, A. C.; Oldenburg, A. L.; Tracy, J. B. Synthesis of Au(Core)/Ag(Shell) Nanoparticles and their Conversion to AuAg Alloy Nanoparticles. *Small* **2011**, *7*, 230−234.

(13) Ma, Y.; Li, W.; Cho, E. C.; Li, Z.; Yu, T.; Zeng, J.; Xie, Z.; Xia, Y. Au@Ag Core−Shell Nanocubes with Finely Tuned and Well-Controlled Sizes, Shell Thicknesses, and Optical Properties. *ACS Nano* **2010**, *4*, 6725−6734.

(14) Maier, S. A.; Atwater, H. A. Plasmonics: Localization and Guiding of Electromagnetic Energy in Metal/Dielectric Structures. *J. Appl. Phys.* **2005**, *98*, 011101−011101−-10.

(15) Samal, A. K.; Polavarapu, L.; Rodal-Cedeira, S.; Liz-Marzán, L. M.; Pérez-Juste, J.; Pastoriza-Santos, I. Size Tunable Au@Ag Core−Shell Nanoparticles: Synthesis and Surface-Enhanced Raman Scattering Properties. *Langmuir* **2013**, *29* (48), 15076−15082.

(16) Jiang, H.-L.; Akita, T.; Ishida, T.; Haruta, M.; Xu, Q. Synergistic Catalysis of Au@Ag Core−Shell Nanoparticles Stabilized on Metal−Organic Framework. *J. Am. Chem. Soc.* **2011**, *133*, 1304−1306.

(17) Endo, T.; Kerman, K.; Nagatani, N.; Hiepa, H. M.; Kim, D.-K.; Yonezawa, Y.; Nakano, K.; Tamiya, E. Multiple Label-Free Detection of Antigen−Antibody Reaction Using Localized Surface Plasmon Resonance-Based Core−Shell Structured Nanoparticle Layer Nano-chip. *Anal. Chem.* **2006**, *78*, 6465−6475.

(18) Yang, Y.; Shi, J.; Kawamura, G.; Nogami, M. Preparation of Au−Ag, Ag−Au Core−Shell Bimetallic Nanoparticles for Surface-Enhanced Raman Scattering. *Scr. Mater.* **2008**, *58*, 862−865.

(19) Jiang, H.-L.; Xu, Q. Recent Progress in Synergistic Catalysis Over Heterometallic Nanoparticles. *J. Mater. Chem.* **2011**, *21*, 13705−13725.

(20) Pande, S.; Chowdhury, J.; Pal, T. Understanding the Enhancement Mechanisms in the Surface-Enhanced Raman Spectra of the 1,10-Phenanthroline Molecule Adsorbed on a Au@Ag Bimetallic Nanocolloid. *J. Phys. Chem. C* **2011**, *115*, 10497−10509.

(21) Tsao, Y.-C.; Rej, S.; Chiu, C.-Y.; Huang, M. H. Aqueous Phase Synthesis of Au−Ag Core−Shell Nanocrystals with Tunable Shapes and Their Optical and Catalytic Properties. *J. Am. Chem. Soc.* **2013**, *136*, 396−404.

(22) Zeng, J.; Zhang, Q.; Chen, J.; Xia, Y. A Comparison Study of the Catalytic Properties of Au-Based Nanocages, Nanoboxes, and Nanoparticles. *Nano Lett.* **2009**, *10*, 30−35.

(23) Sun, Y.; Lei, C. Synthesis of Out-of-Substrate Au−Ag Nanoplates with Enhanced Stability for Catalysis. *Angew. Chem.* **2009**, *121*, 6956−6959.

(24) Bastús, N. G.; Comenge, J.; Puntes, V. c. Kinetically Controlled Seeded Growth Synthesis of Citrate-Stabilized Gold Nanoparticles of up to 200 nm: Size Focusing versus Ostwald Ripening. *Langmuir* **2011**, *27*, 11098−11105.

(25) Pande, S.; Ghosh, S. K.; Praharaj, S.; Panigrahi, S.; Basu, S.; Jana, S.; Pal, A.; Tsukuda, T.; Pal, T. Synthesis of Normal and Inverted Gold−Silver Core−Shell Architectures in β-Cyclodextrin and Their Applications in SERS. *J. Phys. Chem. C* **2007**, *111*, 10806−10813.

(26) Rodríguez-Fernández, J.; Pérez-Juste, J.; García de Abajo, F. J.; Liz-Marzán, L. M. Seeded Growth of Submicron Au Colloids with Quadrupole Plasmon Resonance Modes. *Langmuir* **2006**, *22*, 7007−7010.

(27) Zhang, X.; Wang, H.; Su, Z. Fabrication of Au@Ag Core−Shell Nanoparticles Using Polyelectrolyte Multilayers as Nanoreactors. *Langmuir* **2012**, *28*, 15705−15712.

(28) Chuntonov, L.; Bar-Sadan, M.; Houben, L.; Haran, G. Correlating Electron Tomography and Plasmon Spectroscopy of Single Noble Metal Core−Shell Nanoparticles. *Nano Lett.* **2011**, *12*, 145−150.

(29) Song, Y.; Yang, Y.; Medforth, C. J.; Pereira, E.; Singh, A. K.; Xu, H.; Jiang, Y.; Brinker, C. J.; van Swol, F.; Shelnutt, J. A. Controlled Synthesis of 2-D and 3-D Dendritic Platinum Nanostructures. *J. Am. Chem. Soc.* **2003**, *126*, 635−645.

(30) Wang, L.; Yamauchi, Y. Block Copolymer Mediated Synthesis of Dendritic Platinum Nanoparticles. *J. Am. Chem. Soc.* **2009**, *131*, 9152−9153.

(31) Ataee-Esfahani, H.; Wang, L.; Nemoto, Y.; Yamauchi, Y. Synthesis of Bimetallic Au@Pt Nanoparticles with Au Core and Nanostructured Pt Shell toward Highly Active Electrocatalysts. *Chem. Mater.* **2010**, *22*, 6310−6318.

(32) Wang, L.; Nemoto, Y.; Yamauchi, Y. Direct Synthesis of Spatially-Controlled Pt-on-Pd Bimetallic Nanodendrites with Superior Electrocatalytic Activity. *J. Am. Chem. Soc.* **2011**, *133*, 9674−9677.

(33) Wang, L.; Yamauchi, Y. Autoprogrammed Synthesis of Triple-Layered Au@Pd@Pt Core−Shell Nanoparticles Consisting of a Au@Pd Bimetallic Core and Nanoporous Pt Shell. *J. Am. Chem. Soc.* **2010**, *132*, 13636−13638.

(34) Wang, L.; Yamauchi, Y. Strategic Synthesis of Trimetallic Au@Pd@Pt Core−Shell Nanoparticles from Poly(vinylpyrrolidone)-Based Aqueous Solution toward Highly Active Electrocatalysts. *Chem. Mater.* **2011**, *23*, 2457−2465.

(35) Shi, L.; Wang, A.; Zhang, T.; Zhang, B.; Su, D.; Li, H.; Song, Y. One-Step Synthesis of Au−Pd Alloy Nanodendrites and Their Catalytic Activity. *J. Phys. Chem. C* **2013**, *117*, 12526−12536.

(36) Cacciuto, A.; Auer, S.; Frenkel, D. Onset of Heterogeneous Crystal Nucleation in Colloidal Suspensions. *Nature* **2004**, *428*, 404−406.

21952

dx.doi.org/10.1021/am507391d | *ACS Appl. Mater. Interfaces* 2014, 6, 21946−21953

(37) Liu, L.; Wang, N.; Cao, X.; Guo, L. Direct Electrochemistry of Cytochrome c at a Hierarchically Nanostructured TiO2 Quantum Electrode. *Nano Res.* **2010**, *3*, 369−378.

(38) Pradhan, N.; Pal, A.; Pal, T. Silver Nanoparticle Catalyzed Reduction of Aromatic Nitro Compounds. *Colloid Surface A* **2002**, *196*, 247−257.

(39) Gangula, A.; Podila, R.; M, R.; Karanam, L.; Janardhana, C.; Rao, A. M. Catalytic Reduction of 4-Nitrophenol using Biogenic Gold and Silver Nanoparticles Derived from Breynia rhamnoides. *Langmuir* **2011**, *27*, 15268−15274.

(40) Das, J.; Aziz, M. A.; Yang, H. A Nanocatalyst-Based Assay for Proteins: DNA-Free Ultrasensitive Electrochemical Detection Using Catalytic Reduction of p-Nitrophenol by Gold-Nanoparticle Labels. *J. Am. Chem. Soc.* **2006**, *128*, 16022−16023.

(41) Yan, J.-M.; Zhang, X.-B.; Akita, T.; Haruta, M.; Xu, Q. One-Step Seeding Growth of Magnetically Recyclable Au@Co Core−Shell Nanoparticles: Highly Efficient Catalyst for Hydrolytic Dehydrogenation of Ammonia Borane. *J. Am. Chem. Soc.* **2010**, *132*, 5326−5327.

(42) Quaresma, P.; Soares, L.; Contar, L.; Miranda, A.; Osorio, I.; Carvalho, P. A.; Franco, R.; Pereira, E. Green Photocatalytic Synthesis of Stable Au and Ag Nanoparticles. *Green Chem.* **2009**, *11*, 1889−1893.

(43) Bastús, N. G.; Merkoçi, F.; Piella, J.; Puntes, V. Synthesis of Highly Monodisperse Citrate-Stabilized Silver Nanoparticles of up to 200 nm: Kinetic Control and Catalytic Properties. *Chem. Mater.* **2014**, *26*, 2836−2846.

(44) Wang, D.; Li, Y. Bimetallic Nanocrystals: Liquid-Phase Synthesis and Catalytic Applications. *Adv. Mater.* **2011**, *23*, 1044−1060.

(45) Venkatesan, P.; Santhanalakshmi, J. Designed Synthesis of Au/Ag/Pd Trimetallic Nanoparticle-Based Catalysts for Sonogashira Coupling Reactions. *Langmuir* **2010**, *26*, 12225−12229.

(46) Alayoglu, S.; Nilekar, A. U.; Mavrikakis, M.; Eichhorn, B. Ru-Pt Core-Shell Nanoparticles for Preferential Oxidation of Carbon Monoxide in Hydrogen. *Nat. Mater.* **2008**, *7*, 333−338.

(47) Nilekar, A. U.; Alayoglu, S.; Eichhorn, B.; Mavrikakis, M. Preferential CO Oxidation in Hydrogen: Reactivity of Core−Shell Nanoparticles. *J. Am. Chem. Soc.* **2010**, *132*, 7418−7428.

(48) Guo, X.; Zhang, Q.; Sun, Y.; Zhao, Q.; Yang, J. Lateral Etching of Core−Shell Au@Metal Nanorods to Metal-Tipped Au Nanorods with Improved Catalytic Activity. *ACS Nano* **2012**, *6*, 1165−1175.

(49) Tokonami, S.; Morita, N.; Takasaki, K.; Toshima, N. Novel Synthesis, Structure, and Oxidation Catalysis of Ag/Au Bimetallic Nanoparticles. *J. Phys. Chem. C* **2010**, *114*, 10336−10341.

(50) Wei, Z.; Sun, J.; Li, Y.; Datye, A. K.; Wang, Y. Bimetallic Catalysts for Hydrogen Generation. *Chem. Soc. Rev.* **2012**, *41*, 7994−8008.

(51) Xia, B.; He, F.; Li, L. Preparation of Bimetallic Nanoparticles Using a Facile Green Synthesis Method and Their Application. *Langmuir* **2013**, *29*, 4901−4907.

(52) Quinten, M. Optical Constants of Gold and Silver Clusters in the Spectral Range Between 1.5 and 4.5 eV. *Z. Phys. B: Cond. Mater.* **1996**, *101*, 211−217.

21953

dx.doi.org/10.1021/am507391d | *ACS Appl. Mater. Interfaces* 2014, 6, 21946−21953